Research Article | Vol. 28, No. 5 / 2 March 2020 / Optics Express 7314
Optics EXPRESS

Carrier-envelope-phase measurement of few-cycle mid-infrared laser pulses using high harmonic generation in ZnO

RICHARD HOLLINGER,[1,2,7] DOMINIK HOFF,[1] PHILIPP WUSTELT,[1] SLAWOMIR SKRUSZEWICZ,[1,2] YINYU ZHANG,[1] HUIPENG KANG,[1,2] DANIEL WÜRZLER,[1] TOM JUNGNICKEL,[1] MATHIEU DUMERGUE,[4] ARJUN NAYAK,[4] ROLAND FLENDER,[4] LUDOVIT HAIZER,[4] MÁTÉ KURUCZ,[4] BALINT KISS,[4] SERGEI KÜHN,[4] ERIC CORMIER,[5] CHRISTIAN SPIELMANN,[1,2,3] GERHARD G. PAULUS,[1,2,3] PARASKEVAS TZALLAS,[4,6] AND MATTHIAS KÜBEL[1,8]

[1]*Institute of Optics and Quantum Electronics, Max-Wien-Platz 1, D-07743 Jena, Germany*
[2]*Helmholtz Institute Jena, Fröbelstieg 3, D-07743 Jena, Germany*
[3]*Abbe Center of Photonics, Friedrich Schiller University, Jena, Albert-Einstein-Straße 6, D-07745 Jena, Germany*
[4]*ELI-ALPS, ELI-HU Non-Profit Ltd., Dugonics tér 13, Szeged 6720, Hungary*
[5]*Université de Bordeaux, CNRS, CELIA, CEA, F-33405 Talence, France*
[6]*Foundation for Research and Technology-Hellas, Institute of Electronic Structure and Laser, GR-71110 Heraklion, Greece*
[7]*richard.hollinger@uni-jena.de*
[8]*matthias.kuebel@uni-jena.de*

Abstract: High-harmonic generation (HHG) in crystals offers a simple, affordable and easily accessible route to carrier-envelope phase (CEP) measurements, which scales favorably towards longer wavelengths. We present measurements of HHG in ZnO using few-cycle pulses at 3.1µm. Thanks to the broad bandwidth of the driving laser pulses, spectral overlap between adjacent harmonic orders is achieved. The resulting spectral interference pattern provides access to the relative harmonic phase, and hence, the CEP.

1. Introduction

In recent years, strong-field laser physics has experienced a shift towards longer wavelengths, i.e., from the near-infrared to the mid-infrared (mid-IR) spectral range. On one hand this shift is motivated by the beneficial scaling law of the ponderomotive energy $U_p \sim \lambda^2$ [1,2]. As a result, electrons can be accelerated to very high kinetic energies, even at moderate field strength. Using mid-IR wavelength drivers, this has led to the demonstration of bright x-ray sources [3], soft x-ray attosecond pulses [4,5] high-resolution laser-induced electron diffraction [6,7] and a long-living, keV-temperature, high-charge-state plasma [8]. On the other hand, the low linear excitation rate of mid-IR light in wide band gap semiconductor and dielectric materials allows for applying electric fields nearly as strong as the the critical electric field strength [9,10]. This allows for transitioning from conventional non-linear optics to strong-field physics in solids without inflicting optical damage to the sample [11]. This transition is marked by non-perturbative high harmonic generation (HHG) in solids [12–17], including an HHG plateau, analogous to gases [18].

#383484 https://doi.org/10.1364/OE.383484
Journal © 2020 Received 19 Nov 2019; revised 26 Jan 2020; accepted 27 Jan 2020; published 26 Feb 2020

Optics EXPRESS

Accompanying the discovery of new physical phenomena tremendous progresses has been achieved improving the performance of mid-IR laser sources. Pulse energies up to tens of milli-joules [19], high repetition rates [20,21] and pulse durations down to a few optical cycles [19–23] are now available. Approaching the few cycle regime makes precise control over the carrier envelope phase (CEP) necessary [24]. CEP measurement is typically achieved using an f-2f-Interferometer, where an octave spanning fundamental spectrum is overlapped with its second harmonic signal. In the spectral overlap region, a fringe pattern reveals the *relative* CEP [25,26]. With mid-IR pulses, however, the overlap region between the fundamental and second harmonic may lie outside the detection range of well-developed and affordable Silicon based detectors. Some drawbacks of the f-2f interferometer can be overcome by the stereographic above-threshold ionization (Stereo-ATI) technique for single-shot measurements of the *absolute* CEP [27–29]. While the Stereo-ATI has been demonstrated to work up to the short-wave infrared [30], its application in the mid-IR has been hampered due to the unfavorable scaling of the recollision probability with increasing wavelength [31,32]. More recently, new techniques for determining the CEP of few-cycle pulses under ambient laboratory conditions have been demonstrated [33,34].

Here, we present measurements of HHG in ZnO using few-cycle laser pulses in the mid-IR (3.1 µm). We show that the interference between adjacent harmonic orders delivers a fringe pattern [35], from which the relative CEP can be readily extracted. Importantly, our scheme scales well towards longer wavelengths, where higher harmonic orders can be achieved. Our approach represents a simple and cost-effective method for measuring the relative CEP, and could be easily integrated into a CEP stabilization scheme.

2. Experimental approach

The experiments were carried out using the MIR laser at ELI-ALPS, which provides laser pulses centered around 3.1 µm at a repetition rate of 100 kHz. The output 140 µJ pulses from the optical parametric chirped pulse amplification (OPCPA) system [36] is compressed to ~25 fs (ca. 2.5 optical cycles) using non-linear spectral broadening in a 2 mm thick yttrium aluminum garnet (YAG) crystal [19,22,23] and a 1 mm thick Si plate, followed by a BaF_2 wedge pair. The CEP of the laser pulses is passively stable and additionally actively stabilized and controlled by an acusto-optical phase modulator (Fastlite, Dazzler) which receives feedback from an f-2f interferometer in combination with a CEP measurement processing unit (Fastlite, Fringezz). Besides stabilizing the CEP, the Dazzler can be used to vary the CEP continuously, while the f-2f interferometer monitors the CEP variations.

Figure 1(a) shows a schematic of the experimental setup. The laser pulses are focused by a gold coated concave mirror ($f = 15$ cm) to a spot size of ~200 µm. The peak intensity and field strength were approximately 3 TW/cm^2 and 0.4 V/Å, respectively and clearly below the reported damage threshold value [12]. A 100 µm thick c-cut ZnO crystal (Crystec GmbH) is placed in the focal plane. The generated high harmonic signal was focused to the entrance slit of a UV-VIS spectrometer (Avantes Avaspec ULS3648) by an $f = 5$ cm CaF_2 lens. The integration time was typically 1 ms, which corresponds to averaging over 100 laser shots. A fused silica window was placed after the sample and in front of the spectrometer to avoid focusing intense mid-IR light onto the entrance slit of the spectrometer. All experiments were carried out at room temperature and ambient atmosphere (21.5°C, 45% relative humidity). In addition, measurements with the 134 fs pulses were performed, using 500 µm thick non-centrosymmetric a-cut ZnO as a target. The laser spectra with and without post-compression are shown in Fig. 1(b).

Optics EXPRESS

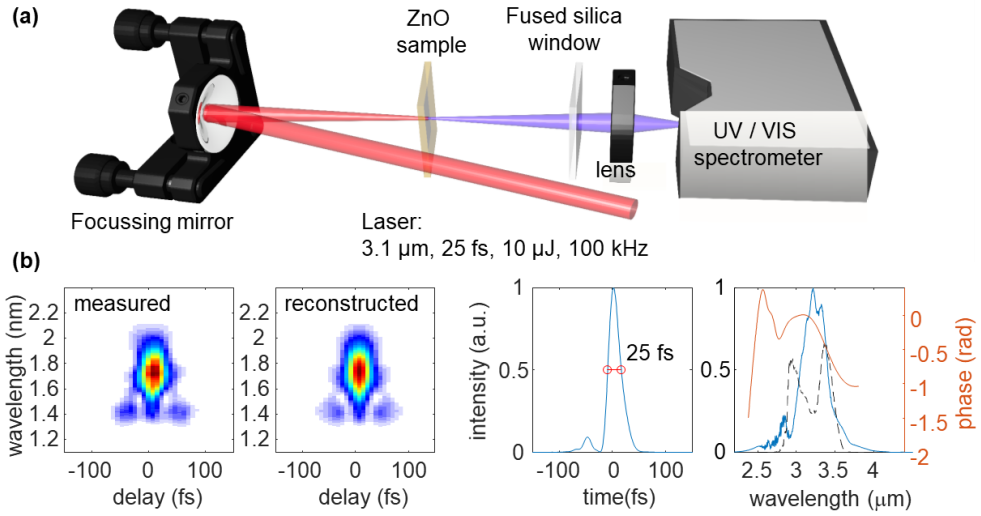

Fig. 1. (a) Experimental setup for CEP measurements in the mid-IR using HHG in ZnO. Mid-IR laser pulses with controllable CEP are focused onto a ZnO crystal. The fundamental laser light is removed using a fused silica window. The high harmonic signal is collected with a CaF_2 lens and detected with a UV-VIS spectrometer. (b) Pulse characterization results using frequency resolved optical gating (FROG). Shown are (from left to right) the measured and reconstructed FROG traces, the retrieved pulse shape in the time domain, and the measured spectrum (blue, solid line) and retrieved spectral phase. The dashed black line shows the spectrum without spectral broadening.

3. Results and discussion

In Fig. 2(a), a typical recorded spectrum with harmonics up to the 13th order is shown. Using the c-cut crystal, only odd harmonic orders are detected due to the inversion symmetry of the c-cut ZnO crystal [37]. The even orders appear when an a-cut crystal is used. For clarity of the peak structure, we present data for 134 fs pulses.

Figure 2(b) shows the recorded CEP-dependence of the harmonic spectrum. In this measurement, the CEP of the driving laser pulses was varied with a triangular wave using the Dazzler, i.e. a constant slope from 0 to 2π and back. Between all odd harmonics we observe a clear oscillating structure of diagonal lines as a function of the CEP. The variations in the signal strength (vertical features) are attributed to short-term fluctuations of the laser power or pointing. Importantly, with regard to CEP measurements, the CEP-dependent interference pattern is not notably affected by these fluctuations. We attribute this insensitivity to the very similar intensity scaling of adjacent order harmonics in the non-perturbative regime [12]. Moreover, pointing fluctuations do not significantly affect the fringe pattern since different harmonic orders propagate collinearly.

Another pronounced feature of the spectra presented in Fig. 2 consists in the strong modulations of the 5th harmonic, which are independent of CEP. These oscillations result from the interference between the 5th harmonic radiation generated at the front and rear surfaces of the ZnO sample. Thus, the spectral spacing in the 5th harmonic is given by:

$$\Delta\lambda = \frac{\lambda^2}{c\Delta t} = \frac{\lambda^2}{cd}\left(\frac{1}{v_g(\lambda)} - \frac{1}{v_g(\lambda/5)}\right)^{-1} \tag{1}$$

Optics EXPRESS

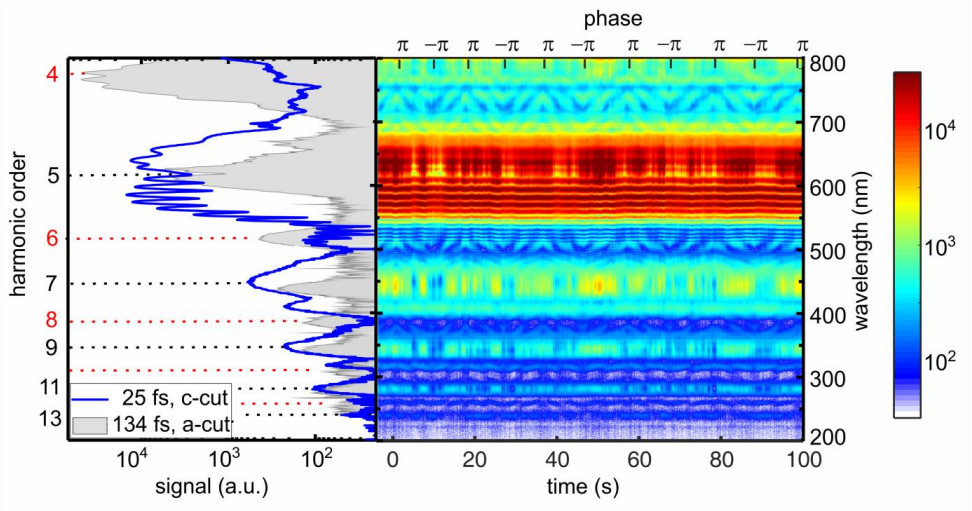

Fig. 2. a) Typical spectrum showing high harmonics of various orders, as indicated. Data is presented using two different crystal geometries and pulse durations, as specified in the legend. b) Measured series of high harmonic spectra using 25fs pulse and a c-cut ZnO crystal, while the CEP is varied using the Dazzler. The colorbar encodes the measured signal strength on a logarithmic scale.

Here d denotes the thickness of the ZnO sample (100 µm), $v_g = \frac{c}{n}\left(1 - \frac{\lambda}{n}\frac{dn}{d\lambda}\right)^{-1}$ the group velocity of the fundamental beam and the 5$^{\text{th}}$ harmonic, n the refractive index and c the speed of light.

Figure 3(a) shows an enlarged view of the 5$^{\text{th}}$ harmonic spectrum, where the change of the variation of the fringe spacing is apparent. Using Eq. (1), the fringe spacing $\delta\lambda(\lambda)$ is calculated and compared to the measurements in Fig. 3(b). The measured and calculated values coincide nearly perfectly, indicating that due to the wide spectrum of the 5$^{\text{th}}$ harmonic the modulation frequency changes over the spectrum. The spectral interference disappears below ~500 nm, due to absorption of the light produced at the front surface of the ZnO crystal. Thus, below 500 nm, only the harmonic light generated at the rear surface reaches the detector.

We now turn towards extracting the CEP from the phase-dependent interference pattern observed in Fig. 2(b). To this end, measurements were performed, in which the CEP was varied in a triangular pattern, Fig. 4(a), and in a sinusoidal pattern, Fig. 4(b). The spectra were recorded using a window filter with transmission in the shown wavelength range. They show the 9$^{\text{th}}$ and 11$^{\text{th}}$ harmonic of the 3.1µm laser, and clear CEP-dependent interference patterns in the vicinity of the harmonics. The triangular and sinusoidal phase variations are clearly imprinted in the interference patterns.

Thanks to the high fringe contrast (up to 3:1) of the interference pattern, the relative phase of adjacent harmonics can be retrieved from individual spectra. This is achieved using a fast Fourier transform of the spectrum in the range (260, 400) nm. The relevant frequency of the interference fringes is identified in the Fourier power spectrum and its phase is unwrapped and plotted in Figs. 4(c) and 4(d) for the triangular and sinusoidal patterns, respectively. The reconstructed phase from the HHG signal (blue line), is compared to twice the CEP measured using the f-2f interferometer at the laser output (red dots). It is important to note that the relative phase of the harmonics with order n and $(n+2)$ varies by $2\Delta\varphi$ when the CEP is changed by $\Delta\varphi$. Therefore, the reconstructed phases in Figs. 4(c) and 4(d) oscillate between 0 and 4π while the CEP was varied between 0 and 2π.

Optics EXPRESS

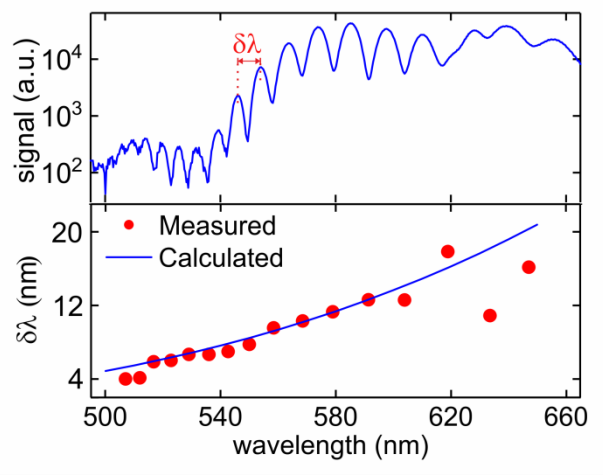

Fig. 3. Spectral interference in the 5th harmonic. (a) Measured spectrum in the vicinity of the 5th harmonic, exhibiting a narrow fringes pattern due to interference between harmonics generated on the front and back surface of the ZnO sample. (b) Measured and calculated (using Eq. (1)) spectral fringe spacing in the 5th harmonic.

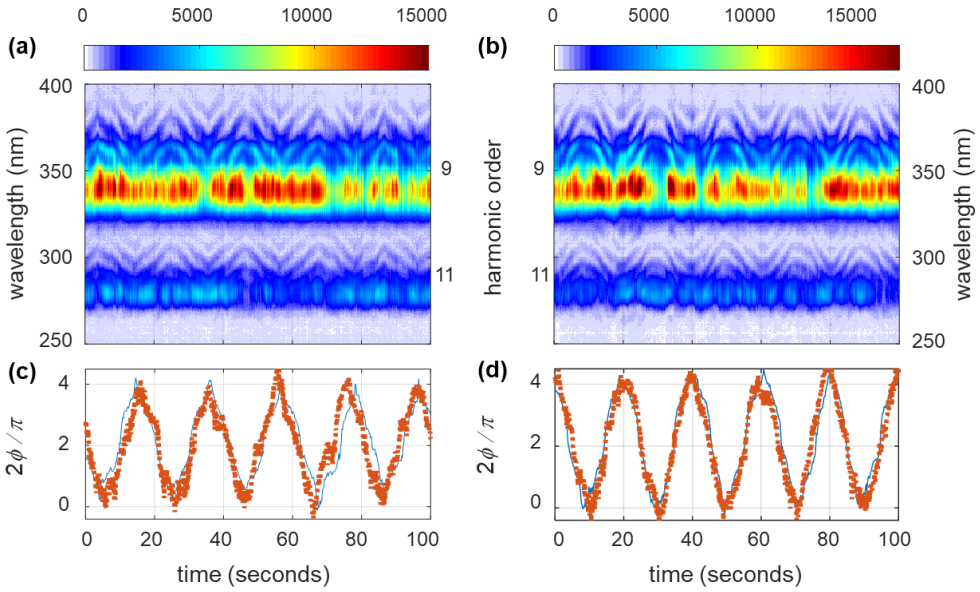

Fig. 4. CEP measurement using HHG in ZnO. Shown are series of spectra in the region around the 9th and 11th harmonic. The CEP of the fundamental pulses is varied in a triangular pattern (a) or a sinusoidal pattern (b) with a frequency of 1/20 Hz. The fringe patterns in between the harmonic signals is used to obtain the relative phase between adjacent odd-order harmonics, which corresponds to twice the CEP ϕ. Panels (c) and (d) show the reconstructed values of 2ϕ (blue solid lines) along with the corresponding values recorded by the f-2f interferometer (red dotted lines).

Optics EXPRESS

The increased sensitivity to CEP variations leads to an ambiguity of π when measuring the CEP via spectral interference of odd order harmonics. This ambiguity could be removed by using non-isotropic media such as a-cut ZnO, where even harmonics can be generated. In that case, the same procedure could be applied to neighboring even and odd order harmonics, whose relative phase varies by $\Delta\varphi$ when the CEP is changed by $\Delta\varphi$. A typical spectrum using a-cut ZnO is shown in Fig. 2(a). CEP-dependent oscillations are observed for a sufficiently broad bandwidth, in between odd and even order harmonics.

We have shown above that the *relative* CEP can be reliably measured using the spectral interferences in the HHG signal. In the following, we utilize this capability to obtain a phase-resolved high harmonic spectrum from the measured data. In Fig. 5, we present the normalized difference, $\frac{S(\phi)-R}{S(\phi)+R}$, between the CEP-dependent harmonic spectra, $S(\phi)$, and the CEP-averaged spectra $R = \frac{1}{2\pi}\int S(\phi)\ d\phi$. This representation of the data shows red and blue areas with pronounced tilts, corresponding the interference fringes between the different harmonic orders. As has been shown in the context of multiphoton ionization [38], the tilts are related to the uncompensated spectral phase in the fundamental spectrum, see Fig. 1. In addition, the yield of the high harmonics exhibits a clear CEP dependence with a π periodicity, as well. Contrary to the interference fringes between the harmonics, the modulations on the maxima of the 9^{th} and 11^{th} harmonics do not exhibit a tilt along the wavelength axis. This suggests that they do not originate in spectral interference but rather in the HHG process itself. Therefore, the modulations in the harmonic yield can be used to determine the *absolute* CEP on target, except for a π ambiguity. For this determination, knowledge over what value of the CEP leads to the maximum harmonic yield is required from theory.

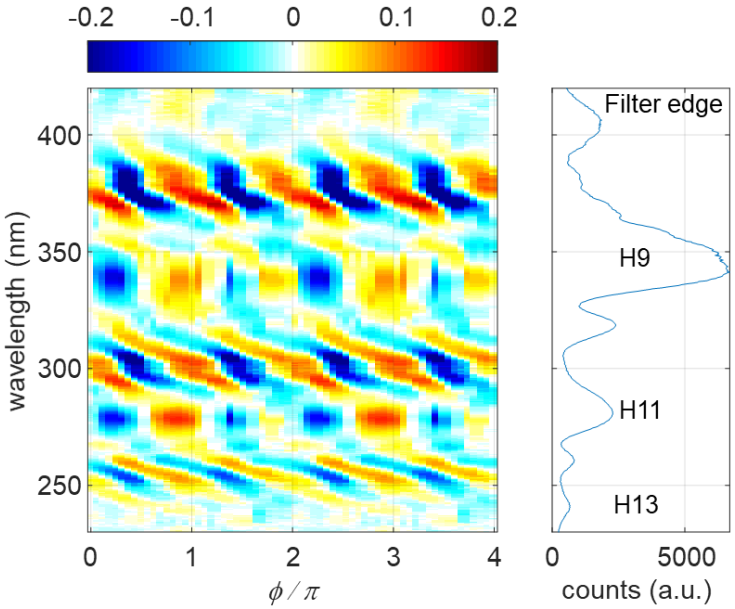

Fig. 5. CEP dependence of the high harmonic spectrum generated by a few-cycle laser pulses at 3.1 µm. The color code denotes the normalized difference between the signal obtained at a given CEP and the CEP-averaged signal. The relative CEP ϕ is obtained from the interference fringes between the harmonics using the method described in the text. Harmonic orders and the filter edge near 400 nm are indicated in the spectrum

Optics EXPRESS

We note that the CEP dependence of the HHG process in crystals is not yet well understood, even though it has been investigated in various materials and for different driving laser wavelengths [39–43]. In particular, a shift of the photon energy of high harmonics as a function of the CEP, i.e. a tilt along the wavelength axis, have been reported in GaSe [39], fused silica [41], MgO [40] and Si [43] using THz, NIR and mid-IR few-cycle laser pulses, respectively. A detailed explanation of the origin of the tilt-free modulations observed in our experiments using ZnO is beyond the scope of the present work and will be the topic of further experiments.

4. Conclusion and outlook

In conclusion, we have shown that HHG in solids such as ZnO allows for a simple detection scheme for the CEP of mid-IR laser pulses. Because it is based on the spectral interference of high harmonics of orders $(n, n+2)$ $(n = 3, 5, 7, \ldots)$, it does not require an octave spanning spectrum; rather, a spectrum with a relative bandwidth $\frac{\Delta\lambda}{\lambda} \gtrsim \frac{2}{n}$ is sufficient to obtain overlap between adjacent harmonics of order n or higher. Using non-centrosymmetric crystals further relaxes this condition due to the appearance of even order harmonics. This would also remove the π ambiguity in the CEP measurement but may require usage of a polarizer, because the polarization states of even and odd-order harmonics may be different [44,45]. Similar to its use in an f-2f interferometer, the polarizer would allow for tuning the fringe contrast between even and odd-order harmonics.

The presented approach scales favorably towards longer wavelength, as the amount of overlap between adjacent harmonics increases with the harmonic orders, and longer wavelengths produce higher-order harmonic orders for suitable targets [16]. The possibility to detect the CEP using light in the visible spectral range allows for the use of affordable silicon-based photon detectors, and makes the presented method very economical. In addition, modulations in the harmonic yield would in perspective allow for the measurement of the absolute CEP. With improved signal-to-noise ratio, it is in principle possible to perform single shot measurements of the high harmonic spectra, and thus, measuring the CEP even for lasers, which are not CEP stable.

Finally, the interference patterns between different pairs of harmonics carries information on the "attochirp" [46], i.e. the relative phase of the various harmonics as they are generated. This information could directly reveal the time structure of the harmonic pulses, an important milestone towards attosecond pulse generation from solids [42].

Funding

European Regional Development Fund (GINOP-2.3.6-15-2015-00001); Deutsche Forschungsgemeinschaft (2101, PA730/7); Helmholtz Association.

Acknowledgments

We thank G. Ernotte and M. Taucer for inspiring discussions. We acknowledge technical support by F. Kohl, A. Rose, T. Weber, and the ELI-ALPS staff. We are grateful to the ELI-ALPS user facility for providing access to their laboratories. The ELI-ALPS project (GINOP-2.3.6-15-2015-00001) is supported by the European Union and co-financed by the European Regional Development Fund. Financial support from the Helmholtz Institute Jena and the Deutsche Forschungsgemeinschaft (DFG) for funding through International Research Training Group (IRTG) 2101 and the QUTIF priority program, grant no. PA730/7, is kindly acknowledged.

References

1. B. Wolter, M. G. Pullen, M. Baudisch, M. Sclafani, M. Hemmer, A. Senftleben, C. D. Schröter, J. Ullrich, R. Moshammer, and J. Biegert, "Strong-Field Physics with Mid-IR Fields," Phys. Rev. X **5**(2), 021034 (2015).
2. S. Y. Kruchinin, F. Krausz, and V. S. Yakovlev, "Colloquium: Strong-field phenomena in periodic systems," Rev. Mod. Phys. **90**(2), 021002 (2018).

Optics EXPRESS

3. J. Weisshaupt, V. Juvé, M. Holtz, S. Ku, M. Woerner, T. Elsaesser, S. Ališauskas, A. Pugžlys, and A. Baltuška, "High-brightness table-top hard X-ray source driven by sub-100-femtosecond mid-infrared pulses," Nat. Photonics **8**(12), 927–930 (2014).
4. T. Gaumnitz, A. Jain, Y. Pertot, M. Huppert, I. Jordan, F. Ardana-Lamas, and H. J. Wörner, "Streaking of 43-attosecond soft-X-ray pulses generated by a passively CEP-stable mid-infrared driver," Opt. Express **25**(22), 27506–27518 (2017).
5. A. S. Johnson, D. R. Austin, D. A. Wood, C. Brahms, A. Gregory, K. B. Holzner, S. Jarosch, E. W. Larsen, S. Parker, C. S. Strüber, P. Ye, J. W. G. Tisch, and J. P. Marangos, "High-flux soft x-ray harmonic generation from ionization-shaped few-cycle laser pulses," Sci. Adv. **4**(5), eaar3761 (2018).
6. C. I. Blaga, J. Xu, A. D. Dichiara, E. Sistrunk, K. Zhang, P. Agostini, T. A. Miller, L. F. Dimauro, and C. D. Lin, "Imaging ultrafast molecular dynamics with laser-induced electron diffraction," Nature **483**(7388), 194–197 (2012).
7. B. Wolter, M. G. Pullen, A. T. Le, M. Baudisch, K. Doblhoff-Dier, A. Senftleben, M. Hemmer, C. D. Schröter, J. Ullrich, T. Pfeifer, R. Moshammer, S. Gräfe, O. Vendrell, C. D. Lin, and J. Biegert, "Ultrafast electron diffraction imaging of bond breaking in di-ionized acetylene," Science **354**(6310), 308–312 (2016).
8. Z. Samsonova, S. Höfer, V. Kaymak, S. Ališauskas, V. Shumakova, A. Pugžlys, A. Baltuška, T. Siefke, S. Kroker, A. Pukhov, O. Rosmej, I. Uschmann, C. Spielmann, and D. Kartashov, "Relativistic Interaction of Long-Wavelength Ultrashort Laser Pulses with Nanowires," Phys. Rev. X **9**(2), 021029 (2019).
9. M. Schultze, E. M. Bothschafter, A. Sommer, S. Holzner, W. Schweinberger, M. Fiess, M. Hofstetter, R. Kienberger, V. Apalkov, V. S. Yakovlev, M. I. Stockman, and F. Krausz, "Controlling dielectrics with the electric field of light," Nature **493**(7430), 75–78 (2013).
10. A. Schiffrin, T. Paasch-Colberg, N. Karpowicz, V. Apalkov, D. Gerster, S. Mühlbrandt, M. Korbman, J. Reichert, M. Schultze, S. Holzner, J. V. Barth, R. Kienberger, R. Ernstorfer, V. S. Yakovlev, M. I. Stockman, and F. Krausz, "Optical-field-induced current in dielectrics," Nature **493**(7430), 70–74 (2013).
11. S. Ghimire, G. Ndabashimiye, A. D. DiChiara, E. Sistrunk, M. I. Stockman, P. Agostini, L. F. DiMauro, and D. A. Reis, "Strong-field and attosecond physics in solids," J. Phys. B: At., Mol. Opt. Phys. **47**(20), 204030 (2014).
12. S. Ghimire, A. D. Dichiara, E. Sistrunk, P. Agostini, L. F. Dimauro, and D. A. Reis, "Observation of high-order harmonic generation in a bulk crystal," Nat. Phys. **7**(2), 138–141 (2011).
13. G. Vampa, T. J. Hammond, N. Thiré, B. E. Schmidt, F. Légaré, C. R. McDonald, T. Brabec, and P. B. Corkum, "Linking high harmonics from gases and solids," Nature **522**(7557), 462–464 (2015).
14. G. Ndabashimiye, S. Ghimire, M. Wu, D. A. Browne, K. J. Schafer, M. B. Gaarde, and D. A. Reis, "Solid-state harmonics beyond the atomic limit," Nature **534**(7608), 520–523 (2016).
15. M. Sivis, M. Taucer, G. Vampa, K. Johnston, A. Staudte, A. Y. Naumov, D. M. Villeneuve, C. Ropers, and P. B. Corkum, "Tailored semiconductors for high-harmonic optoelectronics," Science **357**(6348), 303–306 (2017).
16. S. Ghimire and D. A. Reis, "High-harmonic generation from solids," Nat. Phys. **15**(1), 10–16 (2019).
17. N. Tsatrafyllis, S. Kühn, M. Dumergue, P. Foldi, S. Kahaly, E. Cormier, I. A. Gonoskov, B. Kiss, K. Varju, S. Varro, and P. Tzallas, "Quantum Optical Signatures in a Strong Laser Pulse after Interaction with Semiconductors," Phys. Rev. Lett. **122**(19), 193602 (2019).
18. M. Ferray, A. L'Huillier, X. F. Fi, L. A. Lompre, G. Mainfray, and C. Manus, "Multiple-harmonic conversion of 1064 nm radiation in rare gases," J. Phys. B: At., Mol. Opt. Phys. **21**(3), L31–L35 (1988).
19. V. Shumakova, P. Malevich, S. Ališauskas, A. Voronin, A. M. Zheltikov, D. Faccio, D. Kartashov, A. Baltuška, and A. Pugžlys, "Multi-millijoule few-cycle mid-infrared pulses through nonlinear self-compression in bulk," Nat. Commun. **7**(1), 12877 (2016).
20. U. Elu, M. Baudisch, H. Pires, F. Tani, M. H. Frosz, F. Köttig, A. Ermolov, P. S. J. Russell, and J. Biegert, "High average power and single-cycle pulses from a mid-IR optical parametric chirped pulse amplifier," Optica **4**(9), 1024–1029 (2017).
21. T. P. Butler, D. Gerz, C. Hofer, J. Xu, C. Gaida, T. Heuermann, M. Gebhardt, L. Vamos, W. Schweinberger, J. A. Gessner, T. Siefke, M. Heusinger, U. Zeitner, A. Apolonski, N. Karpowicz, J. Limpert, F. Krausz, and I. Pupeza, "Watt-scale 50-MHz source of single-cycle waveform-stable pulses in the molecular fingerprint region," Opt. Lett. **44**(7), 1730–1733 (2019).
22. M. Hemmer, M. Baudisch, A. Thai, A. Couairon, and J. Biegert, "Self-compression to sub-3-cycle duration of mid-infrared optical pulses in dielectrics," Opt. Express **21**(23), 28095–28102 (2013).
23. S. Gholam-Mirzaei, J. E. Beetar, A. Chacón, and M. Chini, "High-harmonic generation in ZnO driven by self-compressed mid-infrared pulses," J. Opt. Soc. Am. B **35**(4), A27–A31 (2018).
24. T. Brabec and F. Krausz, "Intense few-cycle laser fields: Frontiers of nonlinear optics," Rev. Mod. Phys. **72**(2), 545–591 (2000).
25. L. Xu, C. Spielmann, A. Poppe, T. Brabec, F. Krausz, and T. W. Hänsch, "Route to phase control of ultrashort light pulses," Opt. Lett. **21**(24), 2008–2010 (1996).
26. A. Baltuška, T. Udem, M. Uiberacker, M. Hentschel, E. Goulielmakis, C. Gohle, R. Holzwarth, V. S. Yakovlev, A. Scrinzi, T. W. Hänsch, and F. Krausz, "Attosecond control of electronic processes by intense light fields," Nature **421**(6923), 611–615 (2003).
27. G. G. Paulus, F. Lindner, H. Walther, A. Baltuška, E. Goulielmakis, M. Lezius, and F. Krausz, "Measurement of the phase of few-cycle laser pulses," Phys. Rev. Lett. **91**(25), 253004 (2003).

Optics EXPRESS

28. T. Rathje, N. G. Johnson, M. Möller, F. Süßmann, D. Adolph, M. Kübel, R. Kienberger, M. F. Kling, G. G. Paulus, and A. M. Sayler, "Review of attosecond resolved measurement and control via carrier–envelope phase tagging with above-threshold ionization," J. Phys. B: At., Mol. Opt. Phys. **45**(7), 074003 (2012).
29. D. Hoff, F. J. Furch, T. Witting, K. Rühle, D. Adolph, A. M. Sayler, M. J. J. Vrakking, G. G. Paulus, and C. P. Schulz, "Continuous every-single-shot carrier-envelope phase measurement and control at 100 kHz," Opt. Lett. **43**(16), 3850–3853 (2018).
30. Y. Zhang, P. Kellner, D. Adolph, D. Zille, P. Wustelt, D. Würzler, S. Skruszewicz, M. Möller, A. Max Sayler, and G. G. Paulus, "Single-shot, real-time carrier-envelope phase measurement and tagging based on stereographic above-threshold ionization at short-wave infrared wavelengths," Opt. Lett. **42**(24), 5150–5153 (2017).
31. J. Tate, T. Auguste, H. G. Muller, P. Salières, P. Agostini, and L. F. DiMauro, "Scaling of Wave-Packet Dynamics in an Intense Midinfrared Field," Phys. Rev. Lett. **98**(1), 013901 (2007).
32. P. Colosimo, G. Doumy, C. I. Blaga, J. Wheeler, C. Hauri, F. Catoire, J. Tate, R. Chirla, A. M. March, G. G. Paulus, H. G. Muller, P. Agostini, and L. F. DiMauro, "Scaling strong-field interactions towards the classical limit," Nat. Phys. **4**(5), 386–389 (2008).
33. M. Miranda, F. Silva, L. Neoričić, C. Guo, V. Pervak, M. Canhota, A. S. Silva, ÍJ Sola, R. Romero, P. T. Guerreiro, A. L'Huillier, C. L. Arnold, and H. Crespo, "All-optical measurement of the complete waveform of octave-spanning ultrashort light pulses," Opt. Lett. **44**(2), 191–194 (2019).
34. M. Kubullek, Z. Wang, K. von der Brelje, D. Zimin, P. Rosenberger, J. Schötz, M. Neuhaus, S. Sederberg, A. Staudte, N. Karpowicz, M. F. Kling, and B. Bergues, "Single-shot carrier–envelope-phase measurement in ambient air," Optica **7**(1), 35–39 (2020).
35. X. Song, R. Zuo, S. Yang, P. Li, T. Meier, and W. Yang, "Attosecond temporal confinement of interband excitation by intraband motion," Opt. Express **27**(3), 2225–2234 (2019).
36. N. Thiré, R. Maksimenka, B. Kiss, C. Ferchaud, G. Gitzinger, T. Pinoteau, H. Jousselin, S. Jarosch, P. Bizouard, V. Di Pietro, E. Cormier, K. Osvay, and N. Forget, "Highly stable, 15 W, few-cycle, 65 mrad CEP-noise mid-IR OPCPA for statistical physics," Opt. Express **26**(21), 26907–26915 (2018).
37. S. Gholam-Mirzaei, J. Beetar, and M. Chini, "High harmonic generation in ZnO with a high-power mid-IR OPA," Appl. Phys. Lett. **110**(6), 061101 (2017).
38. D. Zille, D. Adolph, M. Möller, A. M. Sayler, and G. G. Paulus, "Chirp and carrier-envelope-phase effects in the multiphoton regime: measurements and analytical modeling of strong-field ionization of sodium," New J. Phys. **20**(6), 063018 (2018).
39. O. Schubert, M. Hohenleutner, F. Langer, B. Urbanek, C. Lange, U. Huttner, D. Golde, T. Meier, M. Kira, S. W. Koch, and R. Huber, "Sub-cycle control of terahertz high-harmonic generation by dynamical Bloch oscillations," Nat. Photonics **8**(2), 119–123 (2014).
40. Y. S. You, M. Wu, Y. Yin, A. Chew, X. Ren, S. Gholam-Mirzaei, D. A. Browne, M. Chini, Z. Chang, K. J. Schafer, and S. Ghimire, "Laser waveform control of extreme ultraviolet high harmonics from solids," Opt. Lett. **42**(9), 1816–1819 (2017).
41. Y. S. You, Y. Yin, Y. Wu, A. Chew, X. Ren, F. Zhuang, S. Gholam-Mirzaei, M. Chini, Z. Chang, and S. Ghimire, "High-harmonic generation in amorphous solids," Nat. Commun. **8**(1), 724 (2017).
42. M. Garg, H.-Y. Kim, and E. Goulielmakis, "Ultimate waveform reproducibility of extreme-ultraviolet pulses by high-harmonic generation in quartz," Nat. Photonics **12**(5), 291–296 (2018).
43. H. Shirai, F. Kumaki, Y. Nomura, and T. Fuji, "High-harmonic generation in solids driven by subcycle midinfrared pulses from two-color filamentation," Opt. Lett. **43**(9), 2094–2097 (2018).
44. T. T. Luu and H. J. Wörner, "Measurement of the Berry curvature of solids using high-harmonic spectroscopy," Nat. Commun. **9**(1), 916 (2018).
45. H. Liu, Y. Li, Y. S. You, S. Ghimire, T. F. Heinz, and D. A. Reis, "High-harmonic generation from an atomically thin semiconductor," Nat. Phys. **13**(3), 262–265 (2017).
46. P. M. Paul, E. S. Toma, P. Breger, G. Mullot, F. Augé, P. Balcou, H. G. Muller, and P. Agostini, "Observation of a Train of Attosecond Pulses from High Harmonic Generation," Science **292**(5522), 1689–1692 (2001).